Physics of Semiconductors. Semiconductor Physics

UDC 536.42+539.19 DOI: 10.33910/2687-153X-2020-1-3-113-122

Comparative analysis of semiconductor-metal phase transition mechanisms in vanadium oxides (V_2O_3 and VO_2)

A. V. Ilinskiy✉[1], E. I. Nikulin[1], E. B. Shadrin[1]

[1] Ioffe Institute, 26 Politekhnicheskaya Str., Saint Petersburg 194021, Russia

Authors

Aleksandr V. Ilinskiy, e-mail: Ilinskiy@mail.ioffe.ru

Evgeniy I. Nikulin

Evgeniy B. Shadrin, ORCID: 0000-0002-1423-2852

For citation: Ilinskiy, A. V., Nikulin, E. I., Shadrin, E. B. (2020) Comparative analysis of semiconductor-metal phase transition mechanisms in vanadium oxides (V_2O_3 and VO_2). *Physics of Complex Systems*, 1 (3), 113–122. DOI: 10.33910/2687-153X-2020-1-3-113-122

Received 31 May 2020; reviewed 6 July 2020; accepted 6 July 2020.

Abstract. In this study, phase transformation mechanisms in thin V_2O_3 and VO_2 films are analysed based on experimental data and on the qualitative model for vanadium oxides proposed by the authors of the study. New features of semiconductor-metal phase transformation mechanism revealed in V_2O_3 are discussed. Characteristics of phase transition process in V_2O_3 is compared with the features of a similar phase transformation in thin VO_2 in detail.

Keywords: vanadium oxides, Magneli phases, semiconductor-metal phase transition, phase transformations, correlation energy.

Introduction

Recently, there has been a revival of interest in studying Semiconductor-Metal Phase Transition (SMPT) in vanadium oxides in the Magneli series: VO_2, V_2O_3, V_6O_{13}, V_3O_5, V_4O_7, V_6O_{11}, etc. This interest is due to unusual results for vanadium dioxide obtained using modern research methods: optical, femtosecond and dielectric spectroscopy (Wegkamp, Stähler 2015; Ilinskiy et al. 2020), spectroscopy of vanadium-oxide photonic crystals (Fan et al. 2015; Golubev et al. 2001; Lu, Zhao 2012; Ye et al. 2015), atomic force microscopy (Tselev et al. 2013), micro-Raman light scattering (Schilbe 2002) and others. Such studies have resulted in a comprehensive understanding of the processes that occur during phase transition in vanadium oxides.

However, such comprehensive understanding only exists for vanadium dioxide. Analysis of the mechanisms of phase transformations in other oxides of the Magneli series has to a large extent been neglected by researchers. Therefore, in this work, the main focus is on vanadium sesquioxide (V_2O_3), a compound possessing a number of unusual physical properties. It seems reasonable to consider these unusual properties by comparing them with the properties of the well-studied VO_2 (temperature SMPT T_c = 340 K).

SMPT also occurs in V_2O_3 with increasing temperature, but it occurs at lower temperatures than in VO_2 (at T_c = 140 K < T_c = 340 K). Moreover, the increase in the electrical conductivity of V_2O_3 after phase transition is much larger (for a single V_2O_3 crystal, the change is 7 orders of magnitude, and in VO_2 it is 4 orders of magnitude). There is no doubt that these differences are associated with differences in vanadium oxide crystal structure. It is crucial to note that vanadium atom has an unfinished

d-shell, and also that strong interactions between electrons play an important role in the phase transition when the energy structure of the crystal is rearranged.

Namely, a strong temperature dependence of the semiconductor energy gap width is associated with correlation effects in V_2O_3 and VO_2 compounds (Gatti et al. 2007). In such materials, the position of energy bands depends on their occupancy by electrons. Since V_2O_3 and VO_2 are oxides of V, a transition metal (No. 23 in the periodic table), they exhibit a fundamental property of vanadium: the dependence of the energy position of atomic levels on their electron occupancy. This conclusion is confirmed by the analysis of electronic configurations of Ti, V, and Cr, i.e. elements located in the 4th period of the table.

Namely, during the transition from element 22 (Ti with $3d^2 4s^2$ configuration) to element 23 (V with $3d^3 4s^2$ configuration), the 3*d* shell is filled with electrons. But when going to element 24 (Cr: $3d^5 4s^1$), the filling sequence is violated. This is due to the fact that the additional electron acquired by Cr greatly reduces the energy of the 3*d* level and initiates a transition of an electron from the 4*s* level to the 3*d* level. The reasons for the lower 3*d* level energy in V and Cr atoms are the strong interactions between the electrons. These interactions take place simultaneously with the interaction of electrons with the V nucleus. The ability of V levels to lower energy when they are occupied by electrons is transferred to vanadium oxides, in which the positions of the bands on the energy scale are also dependent on their electron occupancy.

Despite the persuasiveness of these arguments, the specific details of V_2O_3 and VO_2 electronic spectrum and crystal structure transformation during the phase transition are of great interest, and for V_2O_3 they still remain unclear.

The objective of this work, therefore, was to study the features of the phase transition in nanocrystallites of thin V_2O_3 films in detail, as well as to compare these features with well-studied features of SMPT in thin VO_2 films.

General information on the physical properties of V_2O_3 and VO_2 single crystals

Vanadium sesquioxide V_2O_3

The V_2O_3 crystal lattice is a corundum (Al_2O_3) type lattice (Tan et al. 2012). The unit cell of the rhombohedral (trigonal) phase contains 4 vanadium atoms and 6 oxygen atoms (V_4O_6). In the V_2O_3 lattice, for every two oxygen octahedra containing V^{3+}, one octahedron does not contain the V^{3+} ion. Such octahedra with empty bases are located on both sides of a pair of octahedra with filled bases. The coordination number of the V^{3+} ion is 6, the coordination number of the O^{2-} ion is 4.

In V_2O_3 single crystals, SMPT occurs at an increased temperature of T_c = 140 K. In this case, single crystal symmetry rises from monoclinic to rhombohedral (trigonal) (Nagaosa et al. 2010). The band gap in the semiconductor low-temperature phase is estimated at E_g = 0.3 eV (Keller et al. 2004).

Vanadium Dioxide VO_2

The crystal lattice of the VO_2 metal phase has tetragonal symmetry, while the semiconductor lattice has monoclinic symmetry (Shimazu et al. 2015). The unit cell contains 2 vanadium atoms and 4 oxygen atoms, (V_2O_4). In the VO_2 lattice, all oxygen octahedra contain vanadium atoms in the centres of their bases. The coordination number of the V^{4+} ion is 6, the coordination number of the O^{2-} ion is 3.

In vanadium dioxide single crystals, SMPT occurs with the temperature increase to T = 340 K.

The band gap in the semiconductor low-temperature phase is estimated at E_g = 0.7 eV.

SMPT in V_2O_3 and VO_2 films

This work is focused, as indicated above, on the study of phase transition in thin films of vanadium oxides consisting of crystallites with sizes of tens of nanometers. Therefore, when describing the phase transition process, it should be taken into account that the grains of V_2O_3 and VO_2 films have different sizes, which follow a normal distribution. As such, grains differ from each other by the contributions of surface energy to the phase transition process, and, consequently, differ in phase transition temperatures, the width and shape of the elementary hysteresis loops and the degree of grain adhesion to the substrate. It follows that all of the above factors have to be taken into account to describe the SMPT mechanism in nanocrystalline films. At the initial stage of phase transition modelling, this work will only

 DOI: 10.33910/2687-153X-2020-1-3-113-122

discuss the features of SMPT in individual nanocrystallites, while at the final stage it will be possible to make phase transition in the entire film as a whole.

Samples

The samples were thin (about 70 nm thickness) V_2O_3 and VO_2 films synthesized by laser ablation method on a SiAl ceramic substrate. For optical experiments, films synthesized on a mirror aluminum layer preliminarily deposited on a SiAl substrate were used. A thin-film optical interferometer arose. The use of such a thin-film Fabry–Pérot interferometer allows one to enhance the effect of a change in the reflection coefficient of the film structure during a phase transition.

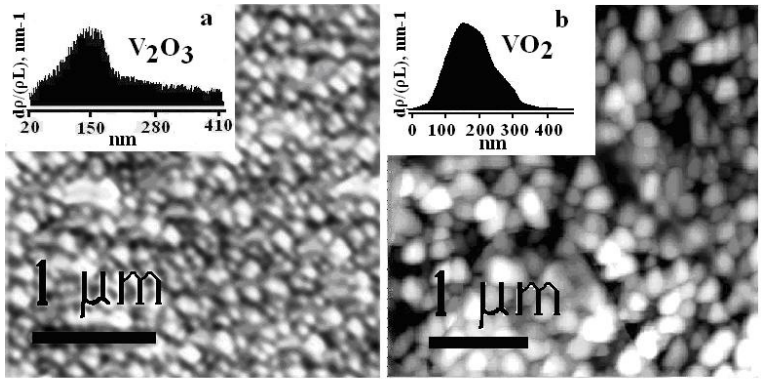

Fig. 1. The atomic force image of V_2O_3-a and VO_2-b films

Figure 1 shows the AFM images of V_2O_3 and VO_2 films. A comparison of the images shows that the films have a uniform granular structure with a typically occurring grain size of 150–200 nm. At the same time, histograms show that the grain size of the films is distributed. The shape and width of the temperature hysteresis loops of the films as a whole depends on the size distribution.

The results of the experiments

Temperature hysteresis loops of the electrical conductivity of films

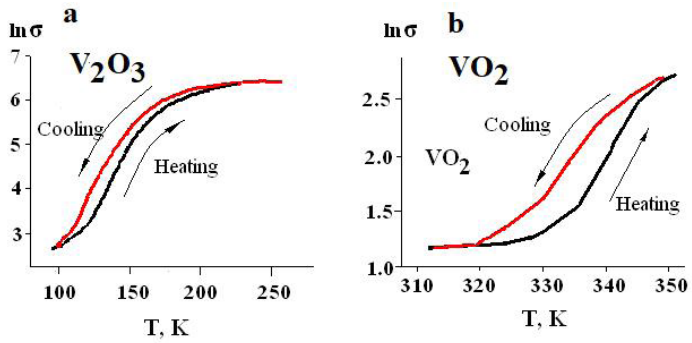

Fig. 2. The temperature hysteresis loops σ of the film V_2O_3-a, and VO_2-b

Figure 2a shows temperature dependence of electrical conductivity (lnσ(T)) of the V_2O_3 film obtained by us. The graphs show that electrical conductivity of the film increases by more than an order of magnitude with an increase in temperature from 100 to 300 K. At high temperatures, the conductivity is metallic with a weak decrease of conductivity with increasing temperature deep into the metal phase. This is typical of metals. In the heating-cooling cycle, a hysteresis loop extended in temperature is observed (the length of the loop branches is ~120 K). The width of the loop is 7 K, the *centre of gravity* of the branch of the loop corresponding to heating falls onto the temperature T_c = 140 K. This temperature is to a first approximation taken as the temperature of SMPT.

A detailed analysis shows that the value of T_c depends on the size of the crystallites of the film and the degree of imperfection of their crystal structure. Specifically, due to the size distribution of grains, they differ in the widths of the elementary hysteresis loops out of which the main loop is composed. The difference in loop widths indicates the martensitic nature of SMPT in V_2O_3. In addition, a difference in the degree of defectiveness of the grains, for example, a difference in the concentration of oxygen vacancies in film grains, creates a difference in the equilibrium temperatures of the T_c phases in these grains. This is due to the correlation nature of that part of SMPT, which is the Mott electronic phase transition (Gatti et al. 2007). The fact is that oxygen vacancies are electron donors that lower T_c. The shape of hysteresis loop branch, which corresponds to heating and whose *centres of gravity* are taken as the temperature of the phase transition of the film, is determined as the temperature of an infinite percolation conduction cluster formation. It follows that the numerical value of T_c only on average characterizes the temperature of the phase transition in the V_2O_3 film.

It is also important to note here that during the hydrogenation of V_2O_3 film, the entire temperature hysteresis loop shifts toward low temperatures by 4–6 K by the atomic % of embedded hydrogen (Andreev et al. 2017). This circumstance will be used in discussing SMPT mechanisms in the studied film structures.

Figure 2b shows the temperature dependence of the electrical conductivity of VO_2 film. Here, during the phase transition, the electrical conductivity increases by an order of magnitude, and at large T_c temperatures, it is of a metallic nature. But the branches of the hysteresis temperature loop are less extended (30 K), and the loop width is 12 K. Here, when the film is hydrogenated, the entire temperature hysteresis loop shifts toward lower temperatures, but by a larger value than V_2O_3: 10–15 K (Ilinskiy et al. 2011).

Temperature hysteresis loops of film optical reflectivity

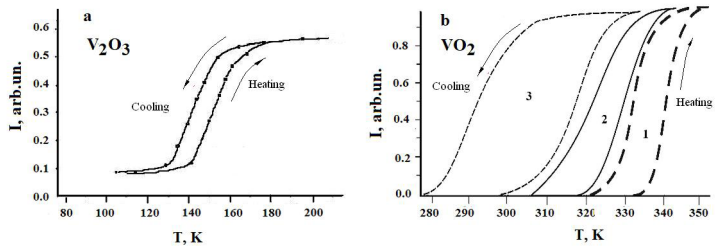

Fig. 3. Temperature hysteresis loops of the intensity of light reflected from films: a — V_2O_3 and b — VO_2 (1 — the initial loop, 2 — after annealing in vacuum for 15 min. at 250°C, 3 — after annealing in vacuum for 15 min. at 350°C)

Figure 3a demonstrates temperature dependence of optical reflectance (I(T)) of the V_2O_3 film obtained by us. The graphs show that the intensity of light reflected from the film increases by more than an order of magnitude with temperature increase from 100 to 300 K. Therefore, we can assume that at high temperatures the film grains are in the metal phase. In the heating-cooling cycle, an intensity hysteresis loop of the light reflected from the film is observed. It is high and extended along temperature (~120 K). The width of the loop is 7 K, the *centre of gravity* of the branch of the loop corresponding to the heating of the sample also falls on the temperature T_c = 140 K.

Figure 3b shows temperature dependence of optical reflectivity of VO_2 film for an *ordinary* film (curve 1). Here, during a phase transition, the intensity of the light reflected from the film increases by an order of magnitude, and at high temperatures the conductivity is metallic. However, the thermal hysteresis loop is less extended in temperature (30 K), and its width is 12 K. In Fig. 3b, loops 2 and 3 were obtained for a film treated in a special way: the film was vacuum annealed. The treating process is described in more detail in the signature to Fig. 3. The figure shows that after this treatment, the hysteresis loops shift to the low-temperature region.

The optical reflectivity of V_2O_3 and VO_2 films is also characterized by the fact that during the hydrogenation of films, all temperature hysteresis loops are shifted toward low temperatures by 10–15 K (Andreev et al. 2017; Ilinskiy et al. 2011).

 DOI: 10.33910/2687-153X-2020-1-3-113-122

Acoustic emission

During SMPT, V_2O_3 and VO_2 films exhibit effective acoustic emission in the immediate vicinity of T_c (Andreev et al. 2000; McBride et al. 1974). This fact is interesting for detailing the processes of phase transformations in these oxides.

Hall constant

For V_2O_3, we measured the Hall constant R_h at low (T = 95 K) and high (T = 300 K) temperatures: R_h = 1200 cm³/K and R_h = 1.3 cm³/K, respectively. For VO_2, the Hall constant obtained by us at low (T = 100 K) and high (T = 380 K) temperatures turned out to be R_h = 6000 cm³/K and R_h = 0.6 cm³/K, respectively. The numerical values of the Hall constant indicate a large increase of the concentration of free electrons in both oxides with increasing temperature.

Discussion of the results

Peierls semiconductor-metal structural phase transition

Peierls phase transition is a change in the symmetry and parameters of the crystal lattice during the formation (destruction) of V-V dimers. Dimer is a system of two V ions coupled in a pair located in neighbouring octahedra. This takes place both in V_2O_3 and in VO_2. Each V ion gives one electron, which is free from the formation of a skeleton, to create a strong σ-bond with the V ion of the neighbouring octahedron in both oxides. Another free electron of the V^{3+} ion, which exists only in V_2O_3, creates, in addition, a strong π-bond with the neighbouring V^{3+} ion. As the temperature decreases (increases), new bonds that are not capable of (destroying) the temperature factor kT arise (disappear) between the atoms of the lattice, i.e., new dimers arise (or are destroyed). When the critical concentration of arising (destroyed) dimers is reached, the symmetry of the entire lattice of the single crystal changes abruptly. The Peierls thermal phase transition in the films of vanadium oxides discussed here has hysteresis with a loop width of the order of several degrees. The large loop width is due to the fact that the small sizes (100–200 nm) of the nanocrystallite films make, according to the Laplace theorem, a significant contribution of surface energy to the energy of SMPT. Namely, the contribution of surface energy to the energy of SMPT is so large that a deviation of several phase equilibrium temperatures T_c is required to complete the phase transition. This effect occurs both when the temperature changes in the direction of the metal phase, and in the direction of the semiconductor phase (Aliev et al. 2006). Let us consider in more detail the process of phase transition in V_2O_3 and VO_2 nanocrystallites.

Vanadium sesquioxide V_2O_3

Figure 4 shows the bases of ten octahedra of the V_2O_3 crystal lattice, in the centres of which V^{3+} ions are located adjacent to each other. These ions form π-bonds between each other due to overlapping $3d_{xz}$-$3d_{x'z}$ and $3d_{yz}$-$3d_{yz}$ branches of vanadium ion orbitals.

The vanadium atom, located in the centre of the base of the oxygen octahedron, forms $3d_{xy}$-bonds with six oxygen atoms due to its $3d^1{}_{xy}(1)3d^0{}_{z2}(1)4s^2(1)4p^0(3)$ hybridization (the superscript is the number of electrons in the orbitals). During the formation of the lattice, a vanadium atom gives on average ½ of its electron density to the oxygen atoms of the environment and turns into a V^{3+} ion. At the same time, each oxygen atom forms four $2s^2(1)2p_x{}^1(1)2p_y{}^1(1)2p_z{}^2(1)$-hybrid orbitals and gives 3/2 of its electron density in connection with vanadium atoms. It forms four complete σ-bonds with vanadium atoms in the centres of the bases of the surrounding octahedra (2 electrons per bond). And the V^{3+} ion creates 6 full-fledged σ-bonds with oxygen ions of its own octahedron. Thus, a strong octahedral V_2O_3 framework is formed.

Since, to ensure the strength of the crystal lattice, each V^{3+} ion gives only 3 electrons to the formation of σ-bonds (one from $3d^1{}_{xy}$ and two from the $4s^2$ orbitals), each V^{3+} ion has two electrons not used to form bonds with O^{2-} ions - octahedron. Due to the participation of one unoccupied electron, a strong σ-bond is formed between $3d_{x2\text{-}y2}$-$3d_{x2\text{-}y2}$ orbitals of V^{3+} ions, which are located at the bases of neighbouring octahedra. Durable $3d_{x2\text{-}y2}$-$3d_{x2\text{-}y2}$ σ-dimers appear in V_2O_3, which are not destroyed either in the semiconductor or in the metal phases (see the lower part of Fig. 4).

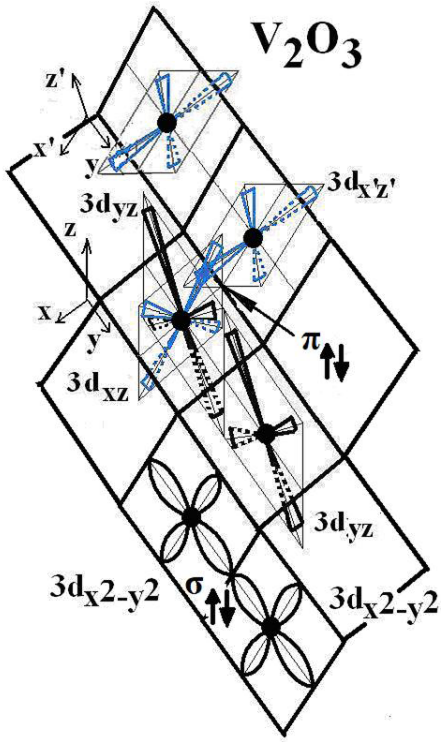

Fig. 4. Fragment of V_2O_3 crystal lattice illustrating the formation of dimers. The upper part of the figure shows the formation at $T < T_c$ of stable π-dimers formed from the dynamic $3d_{xy}$-$3d_{x'y}$s bonds existing at $T > T_c$. The lower part of the figure shows σ-$3d_{x2-y2}$-$3d_{x2-y2}$-dimers stable in V_2O_3 at temperatures both larger and lower than T_c

Electron density corresponding to the second free electron of the V^{3+} ion in the metal phase is uniformly distributed between the $3d_{xz}$ and $3d_{yz}$ orbitals of the vanadium ion in the octahedron. Due to the overlapping branches of the orbitals of the V^{3+} ion of neighbouring octahedra (Fig. 4), V-V pairs arise, connected by π-bonds. A set of such dynamic π-bonds perpendicular to each other creates a one-dimensional zigzag structure along the hexagonal axis C_R, the elements of which are interconnected. Since each V^{3+} ion gives away only one free electron (another is used to create a non-destructive σ-bond), in V_2O_3 there is a system of one-dimensional zigzag filaments created with metallic type conductivity. The value of the Hall constant measured by us unambiguously indicates electronic type of conductivity.

The lattice of the semiconductor V_2O_3 phase has monoclinic symmetry, which contains fewer symmetry elements than the metal phase of rhombohedral symmetry. This is due to the fact that at temperatures lower than T_c, π-dimers are formed. In such dimers, V^{3+} ions are located in the metal phase at the base centres of neighbouring octahedra, which are inclined to each other at an angle of 150°. With SMPT, V^{3+} ions exit base centres and approach each other.

The reason for vanadium ions leaving base centres is that due to the tilt, the overlap of the branches of $3d_{xz}$ and $3d_{x'z'}$- orbitals in $3d_{x'z'}$-$3d_{xz}$-π- bonds is 60% larger than that of $3d_{yz}$-$3d_{yz}$-π-bonds. From this, according to the theory of molecular orbitals, it follows that the binding energy of $3d_{x'z'}$-$3d_{xz}$-π dimers is almost twice as high as the binding energy of $3d_{yz}$-$3d_{yz}$-π dimers, and the distance between the centres of V^{3+} ions is 37% less. The consequence of this is the formation of precisely $3d_{x'z'}$-$3d_{xz}$-π-dimers and a doubling of the repetition period of the peaks of the thermodynamic potential of the one-dimensional system of π-dimers, where C_R. $3d_{xz}$-$3d_{x'z'}$-π-dimers with a higher binding energy than $3d_{yz}$-$3d_{yz}$-π-dimers also capture a single free electron. This excludes the participation of $3d_{yz}$-$3d_{yz}$-π bonds in conductivity. The low-temperature monoclinic phase V_2O_3 acquires sharply reduced conductivity.

In the crystal lattice, the energy levels corresponding to the binding (π) and loosening (π*) of orbitals expand on the energy scale in the π and π* zones, which differ sharply in their energy positions in the conducting and semiconductor phases (Fig. 5). It is crucial that in the semiconductor phase, a gap appears on the energy scale between binding $3d_{xz}$-$3d_{x'z'}$,π-band and binding $3d_{yz}$-$3d_{yz}$-π band (experimentally estimated by Eg = 0.3 eV (Keller et al. 2004)). Thus, the V_2O_3 crystal is in the low-temperature phase a semiconductor with a band gap of 0.3 eV.

 DOI: 10.33910/2687-153X-2020-1-3-113-122

The aforesaid is illustrated in Fig. 5a, which shows a diagram of energy bands of low-temperature V_2O_3 semiconductor phase.

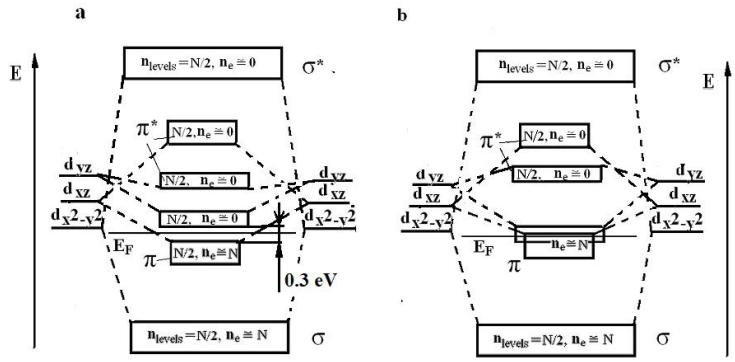

Fig. 5. Diagram of energy zones of V_2O_3 crystal. a — semiconductor phase, b — metal phase

Vanadium Dioxide VO_2

Vanadium V^{4+} ion in each oxygen octahedron, resulting from $3d^1_{xy}(1)3d^1_{z2}(1)4s^2(1)4p^0(3)$ hybridization of vanadium atom, forms 6 σ-bonds with O^{2-} ions, which arise during $2s^2(1)2p_x^1(1)2p_y^1(1)$ hybridization of an oxygen atom. Each oxygen atom is connected by 3—but not 4, as in V_2O_3—σ-bonds with V^{4+} ions, which are located in neighbouring octahedra. The V^{4+} ion gives an average of 4/3 of its electron density to the σ-bond with O^{2-}, which gives an average of 2/3 to the σ-bond. A complete V-O σ-bond arises, having two electrons with oppositely directed spins.

In VO_2 metal phase, each V-octahedron has one free electron per V^{4+} ion, which is not involved in the stabilization of the lattice framework. This electron is located on $3d_{x2-y2}$ orbital, which is located in the plane of the base. The cruciform branches of this orbital are parallel to the ribs of the base of the frame. V^{4+} ions form a system of one-dimensional filaments along the tetragonal axis C_R, which creates a one-dimensional metal-type conductivity in a half-filled energy zone. This zone arises in VO_2 when the energy level corresponding to the $3d_{x2-y2}$ orbitals expands in crystal to zone. The number of energy levels in such zone is equal to the number of V^{4+} ions and, at the same time, is equal to the number of electrons in the zone. Due to Pauli exclusion principle, electrons occupy only half of the levels of the lower part of the zone. The upper half of the zone remains free. This corresponds to the metallic conductivity of the material in high-temperature phase.

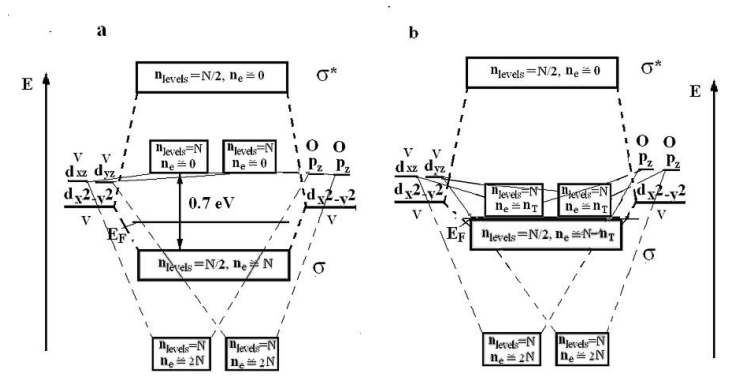

Fig. 6. Diagram of the energy zones of the VO_2 crystal. a — semiconductor phase, b — metal phase

In low-temperature VO_2 phase of monoclinic symmetry a $3d_{x2-y2}$ orbitals of neighbouring octahedra form $3d_{x2-y2}$-$3d_{x2-y2}$ σ-dimers due to the fact that the temperature factor is not enough to destroy them, as it was in the metal phase. Therefore, V^{4+} ions are pairwise shifted towards each other and the period of repetition of the thermodynamic potential along C_R doubles. The crystal conductivity sharply

decreases, and the material acquires semiconductor properties (EG = 0.7 eV), since free electrons are now fixed in $3d_{x2-y2}$-$3d_{x2-y2}$ σ bonds. A structural phase transition to low-symmetry phase occurs.

Fig. 6a is a diagram of the energy zones of low-temperature semiconductor VO_2 phase.

Mott electronic semiconductor-metal phase transition

The Mott phase transition represents a continuous increase in the metallization of a single crystal with an increase of crystal's temperature, which was in a semiconductor state with E_g = 0,7 eV. In this case, a change in the symmetry of the crystal lattice does not occur. With increasing temperature, the concentration of free electrons in the conduction band of the semiconductor continuously increases. The main feature of the Mott phase transition is that experimental data indicates a—very marked— decrease of the band gap of the semiconductor when the transition is completed. When the temperature reaches a critically high value, the energy gap of the semiconductor becomes equal to zero. The semiconductor goes into a metallic state with a lattice that maintains a low symmetry of the semiconductor phase. This second-order phase transition does not have thermal hysteresis. However, in the vanadium oxides studied by us, the Peierls and Mott phase transitions do not occur in the "pure state". The actual situation is more complicated: when the temperature changes, both phase transitions occur. Moreover, they mutually influence each other. Common schemes of the process of making SMPT in V_2O_3 and VO_2 in the first approximation coincide.

The key finding is that in both oxides, electrons obeying the Fermi distribution cannot receive energy greater than 30 meV at temperatures below T_c, which does not allow efficient transfer through the energy gap (0.3 eV for V_2O_3 and 0.7 eV for VO_2) of such a number of electrons that is necessary for the transition of the material from semiconductor into metallic phase. Such transition is possible when a critical number of dimers that stabilize the semiconductor phase are destroyed ($3d_{xz}$-$3d_{x'z'}$-π dimers for V_2O_3 and $3d_{x2-y2}$-$3d_{x2-y2}$-σ-dimers for VO_2). From the bonds of these dimers, there is a transfer of electrons to the allowed band. It follows that V_2O_3 and VO_2 must remain semiconductors even at room temperature. This, however, conflicts with the results of the experiment. The contradiction is eliminated by Mott's fundamental idea, where phase transition energy has to include high correlation energy of interaction between the electrons moving in the periodic potential of the crystal lattice. According to Mott (Mott 1990), the transfer of electrons into the conduction band causes it to lower in energy, which then increases the transfer of new electrons. This causes additional zone lowering, etc. The zone from which the electrons leave, on the contrary, rises in energy (Gatti et al. 2007). It follows that the standard thermal transfer of electrons into the conduction band of a semiconductor from its valence band with increasing temperature causes a decrease in the band gap if correlation interaction between the electrons exists. At the same time, the concentration of electrons in the conduction band increases. This process is a temperature-extended Mott semiconductor-metal phase transition.

Figures 5 and 6 illustrate the aforesaid. They show the energy diagrams of the bands in the semiconductor and metal phases for both vanadium oxides.

This process in both oxides leads to effective destruction of dimers stabilizing the semiconductor phase and which, according to the theory of valence bonds, serve as electron donors. The semiconductor phase in both oxides rapidly passes into the metallic phase (Peierls transition) upon reaching a critical number of destroyed dimers. Thus, in each grain of the vanadium oxide film, Peierls structural transition is initiated by Mott electronic transition. That is, dimers that remain undisturbed cannot keep the crystal lattice in a state of low symmetry. In all grains, the Peierls phase transition occurs at different temperatures—T_c in a defect-free crystal—depending on their size.

The presence of correlation effects is additionally confirmed by the fact that during VO_2 film annealing in vacuum, the hysteresis loops shift to lower temperatures (Fig. 3b, curves 2, 3). Specifically, during vacuum annealing, oxygen vacancies are formed, which are electron donors. Donor electrons pass into the conduction band. Due to correlation effects, the conduction band decreases in energy, while the band gap and T_c narrow. Hydrogenation of the films also leads to the shift in the temperature hysteresis loops toward lower temperatures in both V_2O_3 and VO_2. Indeed, introduced hydrogen, it being an electron donor, transfers free charge carriers to the conduction band, causing additional correlation lowering in energy and a decrease in T_c.

The destruction of π-dimers (V_2O_3) and σ-dimers (VO_2) with increasing temperature leads to a decrease in the number of dimers to a critical level, so that they cannot keep the lattice in a state of low symmetry. After that, an abrupt Peierls structural transition occurs. Vanadium ions move in an avalanche-

 DOI: 10.33910/2687-153X-2020-1-3-113-122

like direction toward the centres of oxygen octahedra under the influence of the valence forces of the oxygen skeleton. All of crystallite dramatically changes its symmetry and size. In both oxides, a strong acoustic emission arises (Andreev et al. 2000; McBride et al. 1974).

Crucially, it should be noted that acoustic emission in single crystals of both oxides is observed after T_c is reached both when the temperature moves deep into the metal phase and after T_c is reached when the temperature moves deep into the semiconductor phase. This directly indicates the displacement of V ions in both phases in a rather wide temperature range (4–5 K in V_2O_3 and 20 K in VO_2). The width of the temperature range depends on the width of the grain size distribution of the film, since SMPT occurs in grains of different sizes at different temperatures.

Conclusion

This work provides a detailed comparison of the mechanisms of SMPT in sesquioxide (V_2O_3) and vanadium dioxide (VO_2). The comparison is based on the analysis of both experimental data obtained by the authors and the data described in scientific literature. In addition to this, a number of points regarding the SMPT mechanism are described for the first time, such as the two types of π-bonds that can arise in V_2O_3, as well as the new types of π-dimers and σ-dimers that can appear. For the first time, the integrated Mott-Peierls character of SMPT in V_2O_3 has been demonstrated and the causes of near SMPT acoustic emission in both oxides were revealed. The reasons for the difference in the numerical values of the conductivity jumps during SMPT in both oxides have been outlined.

A comparative analysis of the SMPT mechanisms in vanadium oxides expands the possibilities of the practical use of vanadium oxide film structures, as it allows the construction of combined systems for memorization, processing, and storing digital information. Such devices will be of a higher quality than older devices due to the reduction of thermal noise at low SMPT temperatures. In addition, detailed information on the SMPT mechanisms in nanocrystallites of vanadium oxide films will improve the synthesis of thin-film vanadium oxide structures that use the martensitic nature of SMPT in practical devices.

References

Aliev, R. A., Andreev, V. N., Kapralova, V. M. et al. (2006) Vliyanie razmera zeren na fazovyj perekhod metall–poluprovodnik v tonkikh polikristallicheskikh plenkakh dioksida vanadiya [Effect of grain size on the metal–semiconductor phase transition in thin polycrystalline films of vanadium dioxide]. *Fizika tverdogo tela — Physics of the Solid State*, 48 (5), 874–879. (In Russian)

Andreev, V. N., Klimov., V. A., Kompan, M. E. (2017) Fazovyj perekhod metall–dielektrik v gidrirovannykh tonkikh plenkakh V_2O_3 [Metal–insulator phase transition in hydrogenated V_2O_3 thin films]. *Fizika tverdogo tela — Physics of the Solid State*, 59 (12), 2413–2415. DOI: 10.21883/FTT.2017.12.45241.174 (In Russian)

Andreev V. N., Pikulin V. A., Frolov D. I. (2000) Akusticheskaya emissiya pri fazovom perekhode v monokristallakh polutoraokisi vanadiya [Acoustic emission during a phase transition in single crystals of vanadium sesquioxide]. *Fizika tverdogo tela — Physics of the Solid State*, 42 (2), 322–325. (In Russian)

Fan, F., Liu, Y., Li, J., Wang, X.-H., Chang, S.-J. (2015) Active terahertz directional coupler based on phase transition photonic crystals. *Optics Communications*, 336, 59–66. DOI: 10.1016/j.optcom.2014.09.068 (In English)

Gatti, M., Bruneval, F., Olevano, V., Reining, L. (2007) Understanding correlations in vanadium dioxide from first principles. *Physical Review Letters*, 99 (26), article 266402. DOI: 10.1103/PhysRevLett.99.266402 (In English)

Golubev, V. G., Davydov, V. Yu., Kartenko, N. F. et al. (2001) Phase transition-governed opal–VO_2 photonic crystal. *Applied Physics Letters,* 79 (14), 2127–2129. DOI: 10.1063/1.1406144 (In English)

Ilinskiy, A. V., Castro, R. A., Pashkevich, M. E., Shadrin, E. B. (2020) Dielektricheskaya spektroskopiya i osobennosti mekhanizma fazovogo perekhoda poluprovodnik–metall v plenkakh VO_2 [Dielectric spectroscopy and the semiconductor–metal phase transition mechanism in doped VO_2 films]. *Fizika i teknnika poluprovodnikov — Semiconductors*, 54 (2), 153–159. DOI: 10.21883/FTP.2020.02.48910.9267 (In Russian)

Ilinskiy, A. V., Kvashenkina, O. E., Shadrin, E. B. (2011) Metallizatsiya gidrirovaniem monoklinnoj fazy v plenkakh VO_2 [Protonic metallization of monoclinic phase in VO_2-films]. *Fizika i teknnika poluprovodnikov — Semiconductors*, 45 (9), 1197–1202. (In Russian)

Keller, G., Held, K., Eyert, V., Vollhardt, D., Anisimov, V. I. (2004) Electronic structure of paramagnetic V_2O_3: Strongly correlated metallic and Mott insulating phase. *Physical Review B: Covering Condensed Matter and Materials Physics*, 70 (20), article 205116. DOI: 10.1103/PhysRevB.70.205116 (In English)

Lu, Z., Zhao, W. (2012) Nanoscale electro-optic modulators based on graphene-slot waveguides. *Journal of the Optical Society of America. Series B*, 29 (6), 1490–1496. DOI: 10.1364/JOSAB.29.001490 (In English)

McBride, S. L., Hutchison, T. S., Murphy, R. (1974) Acoustic emission and the semiconductor — metal transition in vanadium dioxide thin films. *Scripta Metallurgica*, 8 (4), 431–434. DOI: 10.1016/0036-9748(74)90149-5 (In English)

Mott, N. F. (1990) *Metal-insulator transitions*. 2nd ed. London: Taylor and Francis, 286 p. DOI: 10.1002/crat.2170260620 (In English)

Nagaosa, N., Sinova, J., Onoda, S., MacDonald, A. H., Ong, N. P. (2010) Anomalous hall effect. *Reviews of Modern Physics*, 82 (2), 1539–1592. DOI: 10.1103/RevModPhys.82.1539 (In English)

Schilbe, P. (2002) Raman scattering in VO_2. *Physica B: Condensed Matter*, 316–317, 600–602. DOI: 10.1016/S0921-4526(02)00584-7 (In English)

Shimazu, Y., Okumura, T., Tsuchiya, T. et al. (2015) Metal–insulator transition of c-axis-controlled V_2O_3 thin film. *Journal of the Physical Society of Japan*, 84 (6), 64701–64705. DOI: 10.7566/JPSJ.84.064701 (In English)

Tan, X., Yao, T., Long, R. et al. (2012) Unraveling metal-insulator transition mechanism of VO_2triggered by tungsten doping. *Scientific Reports*, 2, article 466. DOI: 10.1038/srep00466 (In English)

Tselev, A., Lavrik, N. V., Kolmakov, A., Kalinin, S. V. (2013) Scanning near-field microwave microscopy of VO_2 and chemical vapor deposition graphene. *Advanced Functional Materials*, 23 (20), 2635–2645. DOI: 10.1002/adfm.201203435 (In English)

Wegkamp, D., Stähler, J. (2015) Ultrafast dynamics during the photoinduced phase transition in VO_2. *Progress in Surface Science*, 90 (4), 464–502. DOI: 10.1016/j.progsurf.2015.10.001 (In English)

Ye, H., Wang, H., Cai, Q. (2015) Two-dimensional VO_2 photonic crystal selective emitter. *Journal of Quantitative Spectroscopy and Radiative Transfer*, 158, 119–126. DOI: 10.1016/j.jqsrt.2015.01.022 (In English)